Composites of $0.3Pb(Mg_{1/3}Nb_{2/3})O_3$–$0.7Pb(Zr_{0.52}Ti_{0.48})O_3$ prepared by a sol–gel method

Dong Soo Paik, S. Komarneni,*† Isaac Robin Abothu and A. V. Prasada Rao

Intercollege Materials Research Laboratory, The Pennsylvania State University, University Park, PA 16802, USA

Lead magnesium niobate (PMN)–lead zirconium titanate (PZT) electroceramic composites have been fabricated from PMN powder + PZT powder (P–P processing) and PMN powder + PZT solution (P–S processing) using a sol–gel process. The particle sizes of PMN–PZT powder prepared by P–S processing were more than three times greater (> 1 μm) in comparison with that of P–P processed powder which was 0.3 μm. The grain size, density, and relative permittivity of PMN–PZT ceramics prepared by P–S processing were larger than those of P–P processed samples. The specimen sintered at 1230 °C by P–P processing exhibited similar properties to the specimen sintered at 1170 °C by P–S processing. Ceramics prepared from a PMN core enclosed in a PZT shell using a polymerized solution mixed at molecular level (powder + solution processing) showed better structural and dielectric properties compared to samples processed with mixed sol–gel powders.

Lead magnesium niobate (PMN) and PMN-based materials have been widely studied for multilayer ceramic capacitors[1] and electrostrictive applications[2] because the assets of PMN are a high relative permittivity, a relatively low sintering temperature, a diffuse phase transformation, and a relatively large strain.[3,4] Because of the above important technological applications[5,6] various compositional modifications of PMN–$Pb(Zr,Ti)O_3$ (PZT) ceramics and their piezoelectric properties have been studied. There has been a great interest in the preparation of pure PMN powders as well as in the sintering and dielectric properties of PMN-based ceramics. Swartz and Shrout[7] studied the correlation between the sintering temperature, grain size and dielectric properties of relaxor ceramics. Duran and co-workers[8] investigated the perovskite phase formation in the PMN–PZT system by a columbite route.

The properties of PMN ceramics mainly depend on the method of preparation and processing conditions.[9] The main problem in making pure PMN ceramics having only a perovskite structure is the formation of cubic and rhombohedral pyrochlore phases such as $Pb_3Nb_4O_{13}$, $Pb_2Nb_2O_7$ and $Pb_5Nb_4O_{15}$.[10,11] It is well known that the presence of these pyrochlore phases, even in small quantities, has a detrimental effect on the dielectric properties of PMN ceramics.[12] Therefore, once a well synthesized PMN powder is achieved it becomes necessary to control other processing parameters in order to obtain adequate and reproducible microstructure and dielectric properties.

Preparation of perovskite PMN by sol–gel processing has been reported[13] in order to eliminate the pyrochlore phase and develop the optimum microstructure and dielectric properties. PZT gel powders prepared by sol–gel processing[14] were easily converted to a pure perovskite phase at low temperatures. Therefore, the preparation methods of PMN–PZT composite powder without the undesirable pyrochlore phase have been widely studied since these solid solution ceramics have good dielectric and piezoelectric properties.[15,16]

This paper focuses on the composite sol–gel processing of the $0.3Pb(Mg_{1/3}Nb_{2/3})O_3$–$0.7Pb(Zr_{0.52}Ti_{0.48})O_3$ system. PMN and PZT solutions were first prepared from which PMN and PZT powders were prepared by hydrolyzing, drying and calcining both of the solutions. In order to make PMN–PZT composites two routes were studied: (*a*) PMN powder was mixed with PZT powder (powder + powder, P–P) and (*b*) PMN powder was added to PZT solution (powder + solution, P–S). The latter composite consists of a PMN core with a PZT shell. The differences in microstructural and dielectric properties of these two types of PMN–PZT powders were investigated.

Experimental

The fabrication procedures of lead magnesium niobate–lead zirconium titanate (PMN–PZT) composite ceramics from PMN powder and PZT solution or powder prepared by traditional sol–gel processing[17,18] are outlined in Fig. 1. Lead acetate trihydrate (99%, Aldrich, Milwaukee, WI) was dissolved in 2-methoxyethanol, and the water of hydration was removed through a series of distillations. Magnesium and niobium ethoxides (98 and 99.95%, Aldrich) were also dissolved in 2-methoxyethanol, and then magnesium–niobium alkoxide solution was prepared after prolonged refluxing to promote formation of the mixed complex alkoxide. The lead solution was added to the magnesium–niobium alkoxide solution and then the solution was refluxed and distilled in order to remove the by-products formed from the reaction solution. The solution of PMN was combined with water and nitric

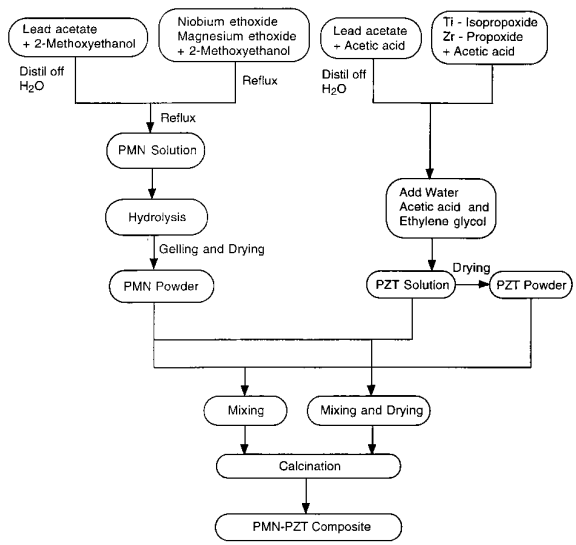

Fig. 1 Flow diagram for sol–gel processing of PMN–PZT powder

† Also with the Department of Agronomy.

acid for hydrolysis. The molar ratios of water to PMN and HNO_3 to PMN are 2 and 0.2 respectively. This procedure resulted in transparent PMN gels. The PZT solution was prepared by an acetic acid based sol–gel processing as described previously.[18] Lead acetate trihydrate was dissolved in acetic acid and then heated to remove the water. The required quantities of solution of zirconium propoxide (70 mass% solution in propan-l-ol, Aldrich) and titanium isopropoxide (97%, Aldrich) were added in a Zr : Ti mole ratio of 52 : 48. In order to obtain a clear and stable solution, distilled water was added in the proportion of 10 mol of distilled water to one mol of lead. The concentration of PZT solution was adjusted by adding propanol to give a 0.5 M solution.

PMN and PZT gel powders were formed by drying the solutions at 140 °C for 48 h. Each powder was also calcined at 850 °C for 2 h (PMN) and at 700 °C for 2 h (PZT) to obtain the perovskite phase. PMN–PZT composite powders were fabricated in two types of processing: (*i*) PMN powder mixed with PZT powder (powder + powder, P–P), (*ii*) PMN powder mixed with PZT solution (powder + solution, P–S) according to the required mole ratio 0.3PMN–0.7PZT and both mixtures were heated at 900 °C for 2 h. The calcined powders were cold-pressed to form disks of 12.7 mm diameter and 1 mm thickness. PMN–PZT ceramics were fabricated at temperatures of 1170, 1200 and 1230 °C for 4 h in closed alumina crucibles and $PbZrO_3$ powder was added to help control Pb stoichiometry in the sample. The samples for dielectric measurements were prepared from the fired pellets by grinding parallel to 0.5 mm thickness, cleaning ultrasonically and making silver paste electrodes by heating at 500 °C. These specimens were designated according to processing conditions and sintering temperature. For example, PP1 denotes ceramic prepared by powder + powder processing and sintering temperature of 1170 °C (Table 1).

Phase identification of powders was performed using a Scintag X-ray diffractometer with Cu-Kα radiation (Model DMC 105, USA). Morphological investigation of the particles and the fractured surface was performed using a scanning electron microscope (Model ISI-DS 130, Akashi Beam Technology Corporation, Japan). Dielectric properties of the specimens were measured semi-continuously at various frequencies in the temperature range of 30–350 °C at a rate of 4 °C min^{-1} during a temperature programmed sequence using an LCR meter (Hewlett Packard 4274A, USA) controlled by a computerized automatic measuring system.

Results and Discussion

Powder characterization

Dried gel powders of PMN and PZT were heat-treated at various temperatures to obtain the perovskite phase. Fig. 2 illustrates the crystalline phases of PMN, PZT and PMN–PZT composite powders. The perovskite phase of PMN powder first appeared at 700 °C, but did not form in abundance. The perovskite phase content of PMN powder increased gradually up to 94% at 850 °C for 2 h. Although higher proportions of perovskite phase occurred using higher calcination temperatures, the pyrochlore phase could not be completely eliminated. PZT gel-derived powder calcined at 700 °C for 2 h was converted to the perovskite phase, *i.e.* at a much lower temperature than for the PMN powder. As previously described, two types of PMN–PZT composite powders were prepared: from PMN powder + PZT powder and PMN powder + PZT solution. These were calcined at 900 °C for 2 h. Each of these powders exhibited the perovskite phase as shown in Fig. 2(c) and (d). The small quantity of pyrochlore phase of PMN as shown in Fig. 2(a) was eliminated from the composite of PMN and PZT perovskite phase. The PZT phase apparently acted as a seed for the PMN and transformed the composite powder to perovskite phase only. This is in agreement with previous observations for a similar composition derived by monophasic sol–gel processing.[13]

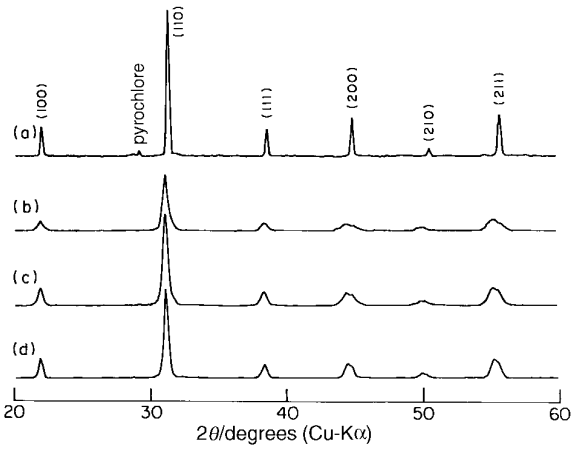

Fig. 2 X-Ray diffraction patterns of sol–gel derived powder: (a) PMN calcined at 850 °C, (b) PZT calcined at 700 °C, (c) PMN–PZT calcined at 900 °C by P–P processing, and (d) PMN–PZT calcined at 900 °C by P–S processing. The materials were soaked for 2 h at each calcining temperature.

Micrographs of the calcined powders derived from P–P and P–S processing are shown in Fig. 3. The P–P powders exhibited a particle size of approximately 0.3 μm. The particle size of the P–S powders was larger at *ca.* 1.2 μm and this powder was highly agglomerated. This increase in particle size is expected in the latter because the solid and solution mixture reacted faster and growth of the particles occurred at 900 °C (Fig. 3).

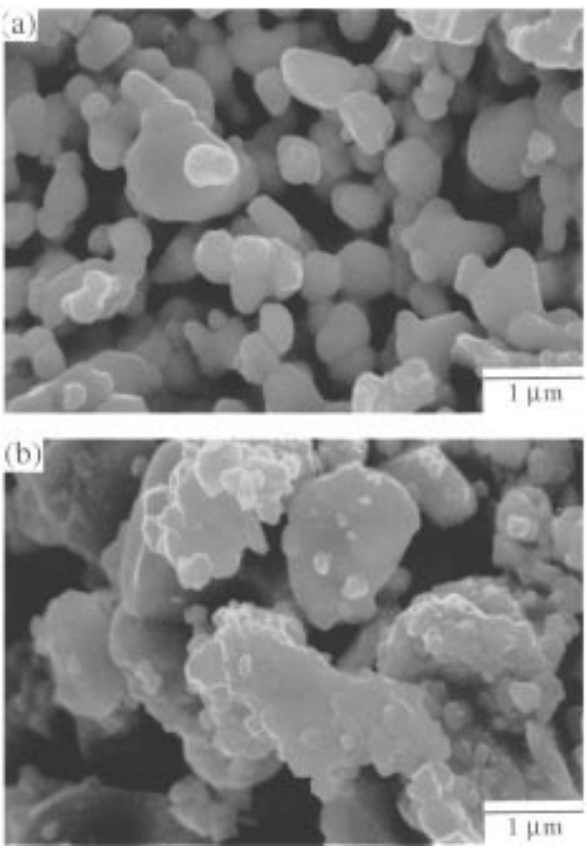

Fig. 3 Microstructure of sol–gel derived powder calcined at 900 °C for 2 h, (a) by P–P processing, and (b) by P–S processing

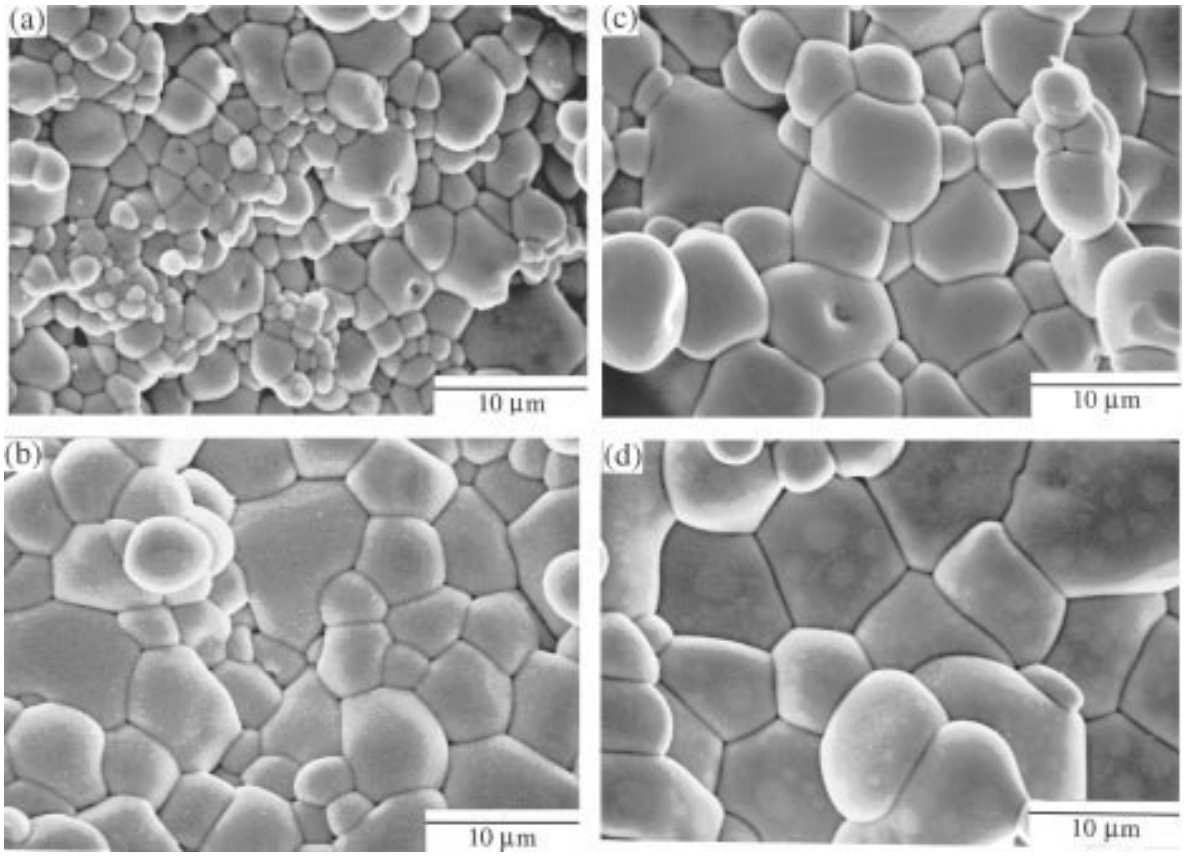

Fig. 4 Microstructure of the fractured surface of PMN–PZT ceramics, (a) sintered at 1200 °C by P–P processing, (b) sintered at 1230 °C by P–P processing, (c) sintered at 1170 °C by P–S processing, and (d) sintered at 1200 °C by P–S processing. The materials were soaked for 4 h at each sintering temperature.

Microstructural properties

Fig. 4 shows the microstructure of the fractured surface sintered at various temperatures for 4 h. They revealed pure perovskite structure and the grain size increased with increasing sintering temperature, as expected, and is summarized in Table 1. Sample PP1 had an average grain size of 1.5 μm at 1170 °C which increased to 5.6 μm [Fig. 4(b)] at 1230 °C. However, the grain sizes in P–P and P–S processed samples were quite different at the same sintering conditions. The average grain size of PS1 was *ca.* 6.4 μm [Fig. 4(c)], which was quite large and uniform compared to that of the P–P processed specimen at the same sintering temperature; the grain size of PS1 at 1170 °C was similar to that of PP3 at 1230 °C. The grain structures prepared by P–S processing were much larger, uniform and denser compared to those of P–P processing. Calcined powder with large particle size led to ceramics with large grains. P–S processing also led to higher densities at lower sintering temperatures.

Schematic diagrams of the two procedures, *i.e.*, P–P and P–S processing of PMN and PZT powders to PMN–PZT composites, are shown in Fig. 5. PMN–PZT ceramics of small grain size formed when PMN and PZT powders were mixed and calcined (P–P processing). When PMN powder of the same size was mixed with a PZT solution (molecular level mixing), the PMN–PZT nanocomposite yielded a larger particle size of *ca.* 1.2 μm. The coating of PZT is responsible for large grain formation because the PZT solution gelled and crystallized rapidly.

The densities of PMN–PZT solid solution ceramics at three different sintering temperatures are listed in Table 1. Densities were higher in P–S processed samples, which is in good agreement with microstructural results shown in Fig. 4. In P–S processing, PMN particles were the cores while PZT solution led to a shell, as shown in Fig. 5. These results clearly show that the efficiency of PMN–PZT solid solution formation can be highly increased depending upon the type of mixing. From the results of microstructure and density, PMN–PZT solid solution ceramics show varying sintering temperatures based on the type of mixing of PMN–PZT powders even though they are prepared from the same starting materials.

Table 1 Sintering temperature (T), density (D), grain size (G), relative permittivity (ε), loss tangent (tan δ) and Curie temperature (T_c) of PMN–PZT ceramics

sample	T/°C	D/g cm^{-3}	G/μm	ε_{max}[a]	tan δ[b]	T_c[a]/°C
PP1	1170	7.37	1.5	6800	0.037	277
PP2	1200	7.42	2.8	11384	0.035	275
PP3	1230	7.61	5.6	18774	0.033	274
PS1	1170	7.70	6.4	26313	0.031	268
PS2	1200	7.72	7.3	27518	0.031	267
PS3	1230	7.70	10.0	25757	0.033	268

[a]At 1 kHz. [b]At 1 kHz and room temperature.

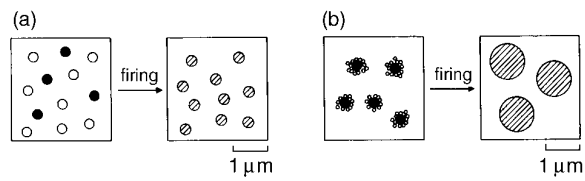

Fig. 5 Schematic diagram of PMN–PZT powder formation: (a) by P–P processing, and (b) by P–S processing (●, PMN particle; ○, PZT particle; ◦, PZT coatings; ▨, PMN–PZT solid solution)

Dielectric properties

The relative permittivity and loss tangent were measured for all the specimens at 0.1, 1, 10 and 100 kHz over a range of temperatures from 30 to 350 °C. Fig. 6 shows relative permittivity *vs.* temperature behavior of sample PP2 at various frequencies. Relaxor materials generally exhibit large and broad dielectric maxima which shift up in temperature with increasing frequency and correspondingly frequency dispersion in the loss tangent is observed as well. However, sample PP2 did not show such frequency dispersion in spite of broad maxima and T_c was essentially constant while the relative permittivity decreased only slightly with increasing frequency. This decrease in relative permittivity with increase in frequency is analogous to behavior found for non-relaxor materials such as $Pb(Zr,Ti)O_3$ and $BaTiO_3$. Samples PP1 and PP2 showed broad maxima but the others showed peak maxima similar to those of typical ferroelectric materials[19] as shown in Fig. 7. No samples exhibited frequency dispersion and differences in relative permittivity and loss tangent were very small. The variations of T_c were also very small (<0.5 °C) at a given frequency range as shown in Fig. 6. Thus, it is concluded that this 30PMN–70PZT composite ceramic is not a relaxor ferroelectric. The relative permittivity of PP samples radically increased with increase in sintering temperature but those of PS samples showed very similar values in the temperature range 1170–1230 °C as shown in Table 1. PS2 sintered at 1200 °C showed a maximum relative permittivity of 27 518 and a maximum density. The grain size of PS3 increased but the relative permittivity and density decreased compared to those

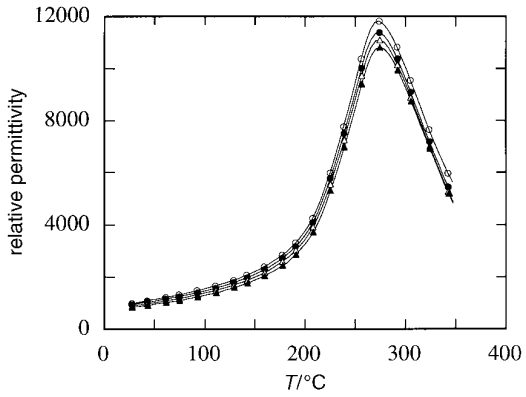

Fig. 6 Relative permittivity *vs.* temperature plot of the specimen prepared by PMN powder + PZT powder processing sintered at 1200 °C for 4 h as a function of frequency (○, 100 Hz; ●, 1 kHz; △, 10 kHz; ▲, 100 kHz)

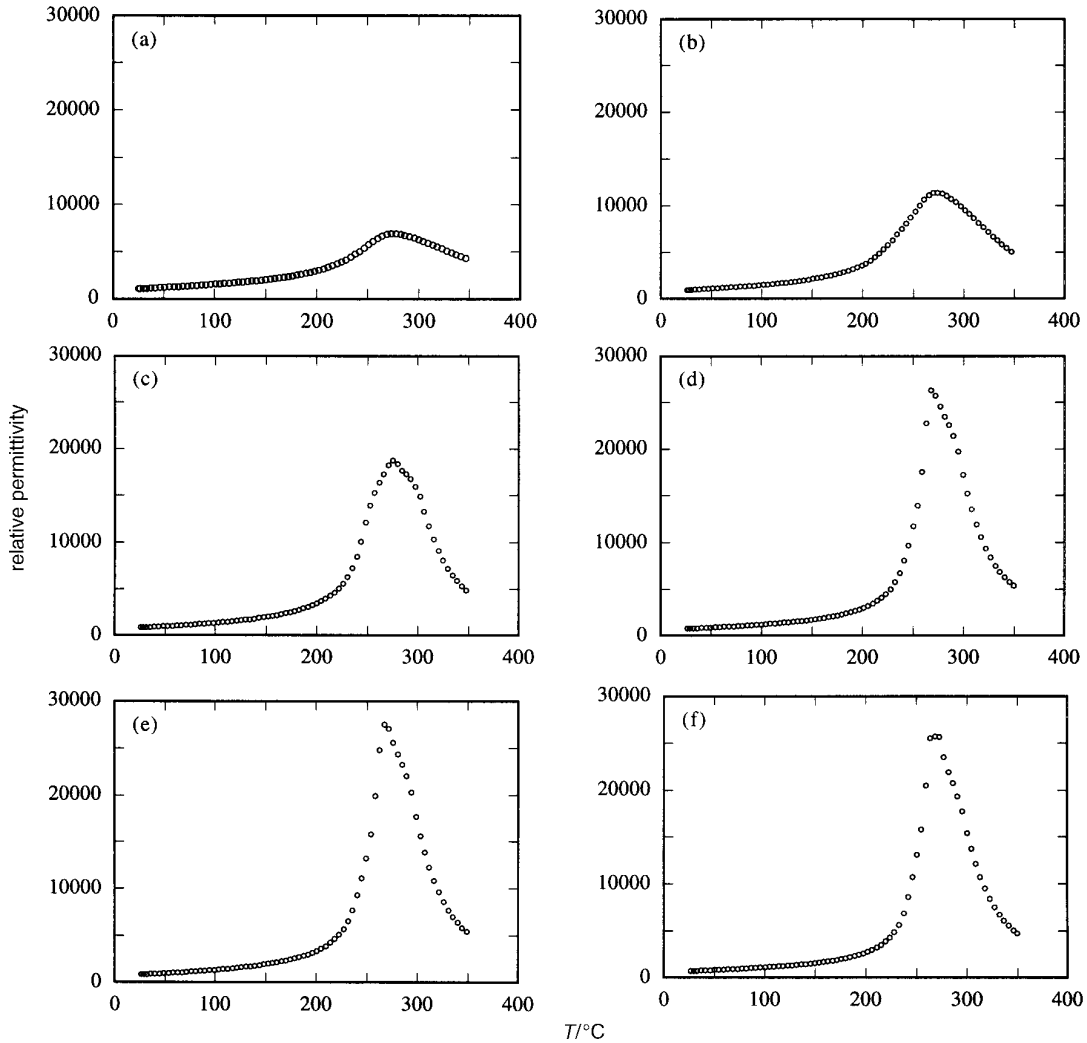

Fig. 7 Comparison of relative permittivity *vs.* temperature plot of PMN–PZT specimens at the measuring frequency of 1 kHz: (a) sintered at 1170 °C by P–P processing; (b) sintered at 1200 °C by P–P processing; (c) sintered at 1230 °C by P–P processing; (d) sintered at 1170 °C by P–S processing; (e) sintered at 1200 °C by P–S processing; (f) sintered at 1230 °C by P–S processing. The materials were soaked for 4 h at each sintering temperature.

of PS2 owing to the higher sintering temperature. The loss tangent was constant from room temperature to the Curie temperature (T_c) and varied in the range 0.007–0.04 for all specimens. The relative permittivities of PP samples were significantly lower than those of PS samples. Among the PP samples, the PP3 sample which was sintered at 1230 °C showed a higher relative permittivity than the other samples sintered at 1170 and 1200 °C. The relative permittivity of PMN–PZT ceramics with grains of >5 μm in size was higher and about twice that of the ceramics with grain size <5 μm and the former samples had a relatively sharp peak phase transition. Increase of the relative permittivity with increase of sintering temperature can be generally explained by the grain size effect. Grain growth takes place to reduce the surface energy during sintering. The area of the grain boundary per unit volume decreases with increasing grain size. Some factors which can degrade the dielectric properties such as space charge layers located in the grain boundary are reduced with grain growth. Also, the mobility of domain walls increases with increased grain growth. Both the above factors lead to an increase of relative permittivity. In other words, the relative permittivity increases with a decrease in space charge layer and an increase in the mobility of the domain walls.[1,20]

This paper has focused on the role of particle size, studying the different particle sizes arising from P–P and P–S processing. The particle size of PMN–PZT powder prepared by P–S processing was large and the ceramics fabricated by this method had denser structure and larger relative permittivity than samples prepared by traditional powder to powder preparation. Values of T_c of the specimens prepared by P–P processing decreased slightly as the sintering temperature increased but specimens prepared by P–S processing showed a T_c of *ca.* 268 °C with no relationship to sintering temperature. The results for P–P samples are in good agreement with those of PMN–PZT based materials which show a decrease of T_c according to increasing grain size and relative permittivity.[9,13] The $0.3Pb(Mg_{1/3}Nb_{2/3})O_3$–$0.7Pb(Zr_{0.52}Ti_{0.48})O_3$ composition has never previously been reported since this composition does not exhibit relaxor behavior as shown above (Fig. 6). Nevertheless, this composition which consists of a large mole ratio of PZT in the PMN–PZT system was selected in order to clearly see the effect of a PMN core enclosed in a PZT shell using a sol–gel polymerized solution. These results clearly showed that the powder + solution processing of the PMN–PZT system has led to enhanced structural and dielectric properties and thus can be adapted to other solid solution systems.

Summary

$0.3Pb(Mg_{1/3}Nb_{2/3})O_3$–$0.7Pb(Zr_{0.52}Ti_{0.48})O_3$ solid solution powder and ceramics have been fabricated with two types of processing, *viz*. PMN powder + PZT powder (P–P) and PMN powder + PZT solution (P–S) processing prepared by a sol–gel method. The results can be summarized as follows.

1 Particle sizes of PMN–PZT powders obtained by P–S processing were increased by more than three times compared to that of P–P processing.

2 A grain size of 7.3 μm was obtained at 1200 °C by P–S processing while P–P processing yielded a grain size of 2.8 μm at the same sintering temperature.

3 The density of ceramics increased by *ca.* 3–5% in P–S processing compared to P–P processing. The relative permittivity at the Curie temperature increased but the loss tangent decreased in P–S processed samples compared to P–P samples.

Structural and dielectric properties of PMN–PZT ceramics which consisted of PMN–PZT powder prepared by a PMN core enclosed in a PZT shell using a sol–gel polymerized solution were superior to those of ceramics prepared by traditional powder to powder processing. Lower sintering temperatures were possible in the fabrication of PMN–PZT ceramics by P–S processing relative to P–P processing.

This work was supported by the division of Materials Research, National Science Foundation under grant No. DMR-9319809.

References

1 S. L. Swartz, T. R. Shrout, W. A. Schulze and L. E. Cross, *J. Am. Ceram. Soc*., 1984, **67**, 311.
2 R. E. Newnham and G. R. Ruschau, *J. Am. Ceram. Soc*., 1991, **74**, 463.
3 L. E. Cross, S. J. Jang, R. E. Newnham, S. Nomura and K. Uchino, *Ferroelectrics*, 1980, **23**, 187.
4 K. Uchino, S. Nomura, L. E. Cross, S. J. Jang and R. E. Newnham, *J. Appl. Phys*., 1980, **51**, 1142.
5 H. Ouchi, K. Nagano and S. Hayagawa, *J. Am. Ceram. Soc*., 1965, **48**, 630.
6 H. Ohuch and M. Nishida, *Ferroelectrics*, 1995, **169**, 309.
7 S. L. Swartz and T. R. Shrout, *Mater. Res. Bull*., 1982, **17**, 1245.
8 M. Villegas, J. R. Jurado, C. Moure and P. Duran, *J. Mater. Sci*., 1995, **30**, 1391.
9 S. M. Gupta and A. R. Kulkarneni, *J. Mater. Res*., 1995, **10**, 953.
10 M. Lejeune and J. P. Bilot, *Ceram. Int*., 1982, **8**, 99.
11 O. Bouquin, M. Lejeune and J. P. Bilot, *J. Am. Ceram. Soc*., 1991, **74**, 1152.
12 J. Chen, A. Gorton, H. M. Chan and P. Harmer, *J. Am. Ceram. Soc*., 1986, **69**, C303.
13 P. Ravindranathan, S. Komarneni, A. S. Bhalla and R. Roy, *J. Am. Ceram. Soc*., 1991, **74**, 2996.
14 U. Selvaraj, K. Brooks, A. V. Prasadarao, S. Komarneni, R. Roy and L. E. Cross, *J. Am. Ceram. Soc*., 1993, **76**, 1441.
15 J. Ho, K. Liu and I. Lin, *J. Mater. Sci*., 1995, **30**, 3936.
16 S. Nomura and K. Uchino, *Ferroelectrics*, 1982, **41**, 117.
17 L. F. Francis, Y. Oh and D. A. Payne, *J. Mater. Sci*., 1990, **25**, 5007.
18 G. Yi, Z. wu and M. Sayer, *J. Appl. Phys*., 1988, **64**, 2717.
19 B. Jaffe, W. R. Cook and H. Jaffe, *Piezoelectric Ceramics*, Academic Press, London and New York, 1971.
20 T. R. Shrout, U. Kumar, M. Megherhi, N. Yang and S. J. Jang, *Ferroelectrics*, 1987, **76**, 479.

Paper 7/01234I; *Received* 21*st February*, 1997